

Planetesimals in Debris Disks

Andrew N. Youdin

George H. Rieke

Steward Observatory, University of Arizona, Tucson, AZ, 85721
youdin@email.arizona.edu, grieke@as.arizona.edu

1. Introduction

Planetesimals form in gas-rich protoplanetary disks around young stars. However, protoplanetary disks fade in about 10 Myr. The planetesimals (and also many of the planets) left behind are too dim to study directly. Fortunately, collisions between planetesimals produce dusty debris disks. These debris disks trace the processes of terrestrial planet formation for 100 Myr and of exo-planetary system evolution out to 10 Gyr. This chapter begins with a summary of planetesimal formation (see Youdin 2010; Chiang & Youdin 2010; Johansen et al. 2015a for more detailed reviews) as a prelude to the epoch of planetesimal destruction. Our review of debris disks covers the key issues, including dust production and dynamics, needed to understand the observations. Our discussion of extrasolar debris keeps an eye on similarities to and differences from Solar System dust.

2. The Formation of Planetesimals

The first step in the accretion of terrestrial planets and gas giant cores is the growth of dust grains into planetesimals, typically defined as solids exceeding a kilometer in size. Models of planetesimal formation have three primary considerations. First, aerodynamic interactions with the gas disk guide the motions of planetesimal building blocks: dust grains, pebbles and boulders.¹ Second, particle sticking and related collisional evolution dominates the early stages of grain growth. Third, the final assembly of planetesimals likely involves particle concentration mechanisms, which ultimately trigger gravitational collapse.

Within a protoplanetary disk, particles drift inward because they encounter a headwind of disk gas, which extracts orbital angular momentum. The headwind arises because gas gets

¹Radiative forces, important in debris disks (§4), are less significant in optically thick protoplanetary disks, where the radiation field is nearly isotropic and gas drag is stronger.

support from radial pressure gradients, an outward acceleration on average. A meter-sized solid falls towards its star on timescales of order 100 years. Getting through the infamous “meter-sized” barrier poses a very stringent constraint on collisional growth (Adachi et al. 1976). Radial drift is fastest for solids that are optimally coupled to the gas, meaning the dimensionless drag constant $\tau_s = \Omega t_{\text{stop}}$ is unity. The stopping time, t_{stop} , is the e-folding timescale for gas drag to damp particle motion, and Ω is the orbital frequency. Larger particles have larger τ_s , but the radial location and disk model also matter. Figure 1 shows that the fastest drifting, $\tau_s = 1$ particles are $\sim 1\text{m}$ around 1 AU and only $\sim 3\text{cm}$ near the Kuiper belt location.

Collisional growth of dust grains up to millimeter sizes is observed in protoplanetary disks (Williams & Cieza 2011). Small bodies stick due to electrostatic interactions, while gravitational attraction becomes important for massive planetesimals. Collisional physics is complex, so laboratory experiments must demonstrate which collision types result in growth versus bouncing, erosion or fragmentation (Blum & Wurm 2008; Beitz et al. 2011). Experiments suggest a mm-sized barrier to growth for silicates (Zsom et al. 2010), although pathways to cm-size and larger bodies by coagulation may exist, especially if ices are present (e.g. Drążkowska et al. 2014). Because cm—m sized solids have low sticking efficiencies and high drift speeds, collisional growth alone may not explain planetesimals.

The gravitational collapse of a sea of small bodies into massive planetesimals offers a top-down alternative to the bottom-up process of collisional growth (Goldreich & Ward 1973; Youdin & Shu 2002). The collapse of (for instance) many cm-sized rocks into a 50 km rubble pile would bypass the meter-size barriers. The key obstacle to gravitational collapse is the mixing of solids by gaseous turbulence (Weidenschilling 1980; Youdin & Lithwick 2007). Collapse is difficult in a smooth (non-clumpy) disk of particles. The aerodynamic concentration of particles into dense clumps helps seed gravitational collapse. Many such concentration mechanisms exist. As an added bonus, collisions in dense particle clumps are gentler and more conducive to coagulation (Johansen et al. 2012).

Particles naturally collect in pressure maxima, which are deviations from the general trend of gas pressure decreasing outwards in disks (Whipple 1972). Inside the pressure maximum, particles are pushed back toward the maximum since the pressure gradient is reversed and particles see a tailwind that reverses the usual inward drift. In principle, particles of all sizes can drift towards and collect inside pressure maxima. However, particles near $\tau_s = 1$ will collect in them fastest, and small $\tau_s \ll 1$ solids can better escape by turbulent diffusion (Lyra & Lin 2013). Many possible sources of pressure maxima exist (see reviews cited above). For instance at ice-lines, the vapor-to-solid transition can also change the ionization state and gas accretion rate, leading to a pressure maximum (Kretke

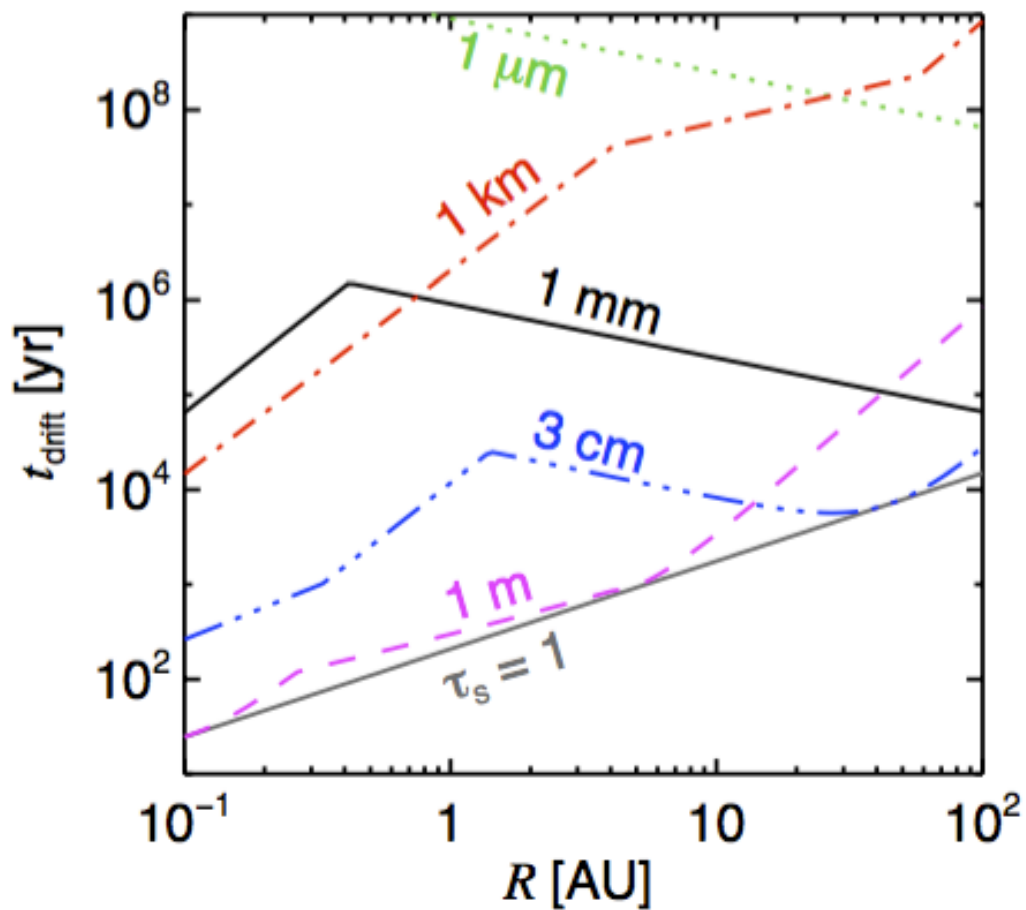


Fig. 1.— The inward radial drift of solids in a gas disk leads to the “meter-size barrier” in planetesimal formation. The drift timescale (t_{drift} , the orbital radius over inflow speed) is plotted against orbital distance in the “minimum mass” disk model of Chiang & Youdin (2010). Curves for various particle sizes are labelled, with kinks at transitions between drag laws. Optimal coupling, the gray $\tau_s = 1$ curve, gives the fastest radial drift.

& Lin 2007). Any such appeal to special locations must explain why planetesimal formation appears so pervasive.

The streaming instability is a powerful aerodynamic particle concentration mechanism, which feeds off radial drift and thus requires no special location (Youdin & Goodman 2005; Johansen & Youdin 2007). That drag forces in disks naturally produce particle clumping is related to a traffic-jam effect, but with many subtleties (Goodman & Pindor 2000; Youdin & Johansen 2007; Jacquet et al. 2011). For strong clumping, the streaming instability requires particle sizes near optimal coupling, $\tau_s \sim 0.1\text{--}1.0$, (Carrera et al. 2015) and a mass ratio of particles-to-gas of $\gtrsim 0.02$; the precise threshold varies with particle sizes and the radial pressure gradient (Bai & Stone 2010). This mass ratio applies to a local patch of the disk ($\sim 10^{-2}$ AU wide) which could be enhanced over the global value by radial drift pileups (Youdin & Chiang 2004). When these conditions are met, particle concentration is incredibly strong and rapid, readily triggering gravitational collapse, as seen in Figure 2, **and producing planetesimals with maximum radii around a few hundred km and with** a wide dispersion of sizes (Johansen et al. 2015b).

A promising route to planetesimals involves particle coagulation into sizes large enough for streaming instabilities to produce clumps that gravitationally collapse into planetesimals. Linking these two mechanisms is a key concern, and gas depletion (increasing τ_s at a given particle size) might be needed in inner disks. In certain conditions, other particle concentration mechanisms could replace the streaming instability. Small particle concentration via the turbulent cascade is an intriguing possibility (Cuzzi et al. 2008), but the ability to produce sufficiently massive planetesimal seeds remains uncertain (Pan et al. 2011).

Finally we return to the possibility of direct gravitational instability (GI) from a smooth background. When drag forces are included, particle GI can occur slowly over long wavelengths, a process known as secular GI (Youdin 2011; Shariff & Cuzzi 2011). More work is needed to understand if secular GI could operate at lower τ_s than streaming instabilities, which would help close any gap between coagulation and dynamical mechanisms. Takahashi & Inutsuka (2014) predicted that long-lived secular GI could explain dust features such as the (since discovered) rings in the HL Tau system, shown in Figure 3.

However planetesimals form in protoplanetary disks, many grow into massive planets, while others do not get that opportunity. In the Solar System, remnant planetesimals and minor planets inhabit the asteroid belt, Kuiper belt, Oort cloud and other stable niches. Low planetesimal surface densities and/or dynamical perturbations from neighboring planets prevent such planetesimal belts from growing into larger planets (Kenyon & Bromley 2012). The prevalence of debris disks confirms that both planetesimal formation and leftover belts of remnant planetesimals are common, as we now describe.

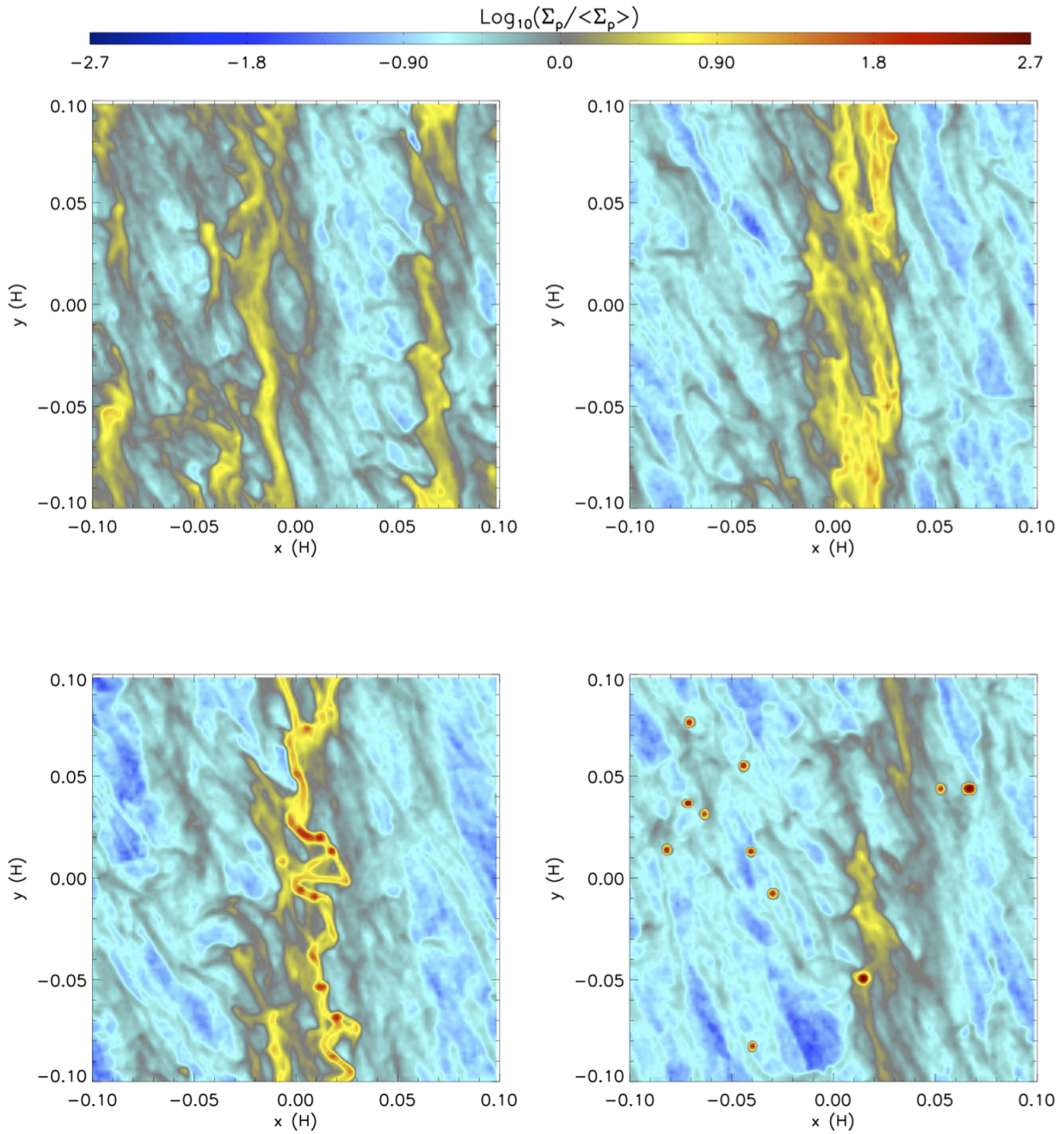


Fig. 2.— Snapshots from a planetesimal formation simulation (Simon et al. 2015). Aerodynamically coupled particles (with $\tau_s = 0.3$) and gas are simulated in a 3D patch of a disk. The particle column density is plotted vs. radius and azimuth (x, y) in units of the gas scaleheight. Time evolves from top-left to bottom-right over 10 local orbits. In the top panels, azimuthally stretched clumps form via streaming instabilities. In the bottom panels, the clumps fragment into planetesimals with masses equivalent to ~ 100 km radii.

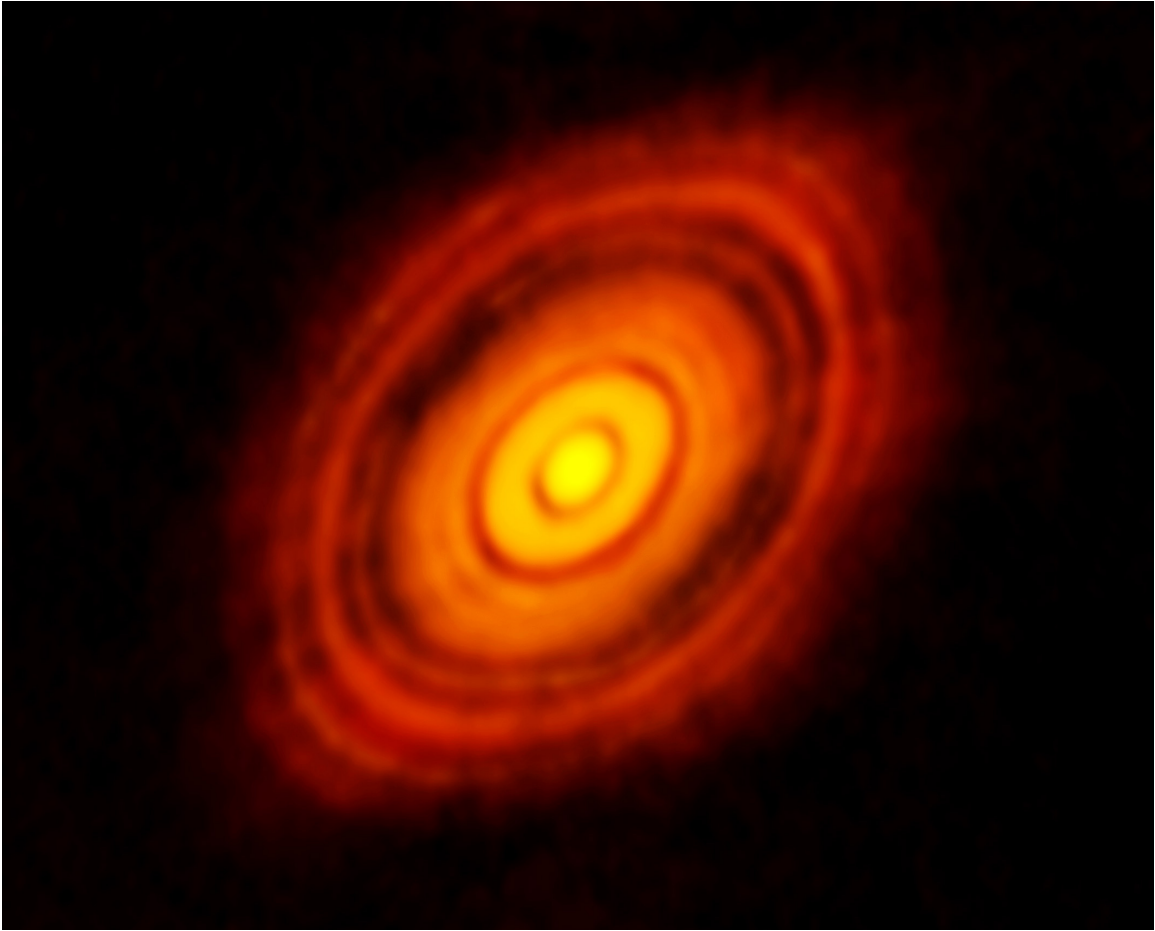


Fig. 3.— The 240 AU diameter protoplanetary disk around the 1 Myr old star HL Tau (ALMA Partnership 2015). ALMA is sensitive to dust grains with radii $\sim 100\mu\text{m}$ –mm. In this image, the central peak is well resolved at roughly 15 AU in diameter. The rings and gaps could be carved by unseen planets or might arise from other dust concentration mechanisms. Credit: ALMA (NRAO/ESO/NAOJ); C. Brogan, B. Saxton

3. Planetesimals and planetary debris disks

The first debris disk was accidentally discovered as infrared excess around the supposedly well-behaved calibration star Vega (Aumann et al. 1984). Astronomers realized they were seeing dust created in planetesimal belts tens of AU from the stars (Weissman 1984; Smith & Terrile 1984). A decade later, the first Kuiper Belt object (other than Pluto and Charon, members of the Kuiper Belt independent of planethood!) was found (Jewitt & Luu 1993), confirming hypotheses that the Solar System had a planetesimal system also at tens of AU from the Sun. This sequence illustrates the importance of debris disks in studying exoplanetary systems, particularly since space-based infrared telescopes, namely *IRAS*, *ISO*, *Spitzer*, *Akari*, *WISE*, and *Herschel*, have found hundreds of them.

Planetesimal collisions in debris disks produce copious amounts of dust through collisional cascades, whereby large planetesimals are gradually ground down to smaller sizes. Rare giant impacts between protoplanets will produce a temporary spike in dust production, while a belt of many smaller planetesimals will erode more gradually. Once dust is ground to micron-sized particles, they are removed by non-gravitational forces. The need to replenish the dust continually is a key difference between evolved debris disks and younger, gas-rich protoplanetary disks. Even modest amounts of dust can dominate the surface area of a planetary system. Dispersing a single 2 km radius planetesimal into micron-sized grains generates a surface area equal to that of all the Solar System planets. This dust is readily detectable in the infrared when warmed by the star, and in the visible by scattered starlight (using a coronagraph to block direct starlight).

4. Dust Production and Evolution in Debris Disks

4.1. Collisional Timescales

Dust production requires frequent collisions. The timescale for planetesimal collisions is

$$t_{c1,2} = \frac{1}{n_2 \sigma_{1,2} v_{1,2}} \approx \frac{2}{N_2 \sigma_1 \Omega}, \quad (1)$$

the time for a “target,” with index 1, to collide with any member of a different-sized “bullet” population, with index 2. The mutual cross section, $\sigma_{1,2}$, is the sum of geometric cross sections in the absence of gravitational focusing, which is weak for high speed destructive impacts (see Youdin & Kenyon 2012, for a review of planet formation processes). The average relative speed, $v_{1,2}$, is also the impact speed when gravitational focusing is weak. With n as the volume density, the volumetric collision rate, $n_1/t_{c1,2}$, is naturally symmetric in particle

species. The second, approximate equality contains N_2 , the vertical column density of bullets, and Ω , the Keplerian orbital frequency. This result assumes that: (1) bullets are smaller than the target so that targets dominate the cross section, σ_1 , while smaller, faster bullets dominate random motions, v_2 ; and (2) compared to eccentricities, orbital inclinations make at least comparable contributions to random motions, giving the scale-height, $H_2 \approx v_2/\Omega$. Thus $N_2 = 2H_2n_2$ gives Equation 1. The removal of uncertain relative speeds makes this result useful.

As an example, consider the Kuiper Belt, with $\sim 0.1M_\oplus$ of planetesimals between 42–48 AU for a surface mass density $\Sigma \approx 1.6 \times 10^{-3} \text{ g cm}^{-2}$ and a typical internal density $\rho = 2 \text{ g/cm}^3$ (Gladman et al. 2001). We assign a uniform radius, $a = 50\text{km}$, to all planetesimals, to overestimate the collision rate between these moderately large KBOs. The resulting collisional timescale, $t_c \approx 800 \text{ Gyr}$, is incredibly long, confirming that impacts between large KBOs do not currently occur.

To illustrate that collision rates are dominated by small bullets, we now consider an idealized size distribution that extends to a maximum radius $a_0 = 50 \text{ km}$ as

$$\bar{n}(a) = N_0 \frac{a_0^{q-1}}{a^q} \propto a^{-q}, \quad (2)$$

with N_0 the surface number density used for normalization. The size distribution $\bar{n}(a)da = dN$ gives the number of bodies (here per unit surface area) in a size bin of width da . The cumulative size distribution $N(> a) \sim \int_a^\infty \bar{n}(a)da \propto a^{1-q}$ for $a \ll a_0$. We adopt $q = 3$, which gives the mass (dominated by the largest bodies) as $\Sigma \approx (4\pi/3)\rho N_0 a_0^3$. The number of objects above a size $a' \ll a_0$ is $N(> a') \approx N_0 a_0^2 / (2a'^2)$. Applying Eq. 1 with $N_2 = N(> a')$ and $\sigma_1 = \pi a_0^2$ gives the collision time for a large (a_0) planetesimals,

$$t_{c1,2} = \frac{16\rho a'^2}{3\Sigma a_0 \Omega} \approx 0.7 \left(\frac{a'}{1 \text{ cm}} \right)^2 \text{ Myr}, \quad (3)$$

showing the domination by small bullets. The ability of small bullets to generate dust debris depends on collision speeds and strength laws.

4.2. Collisional Cascades

Collisional grinding in debris disks leads to a pseudo-steady-state size distribution, reached in $\sim 10\text{--}20 \text{ Myr}$ (Wyatt 2008). The shape of the size distribution depends primarily on impact strength (or disruption threshold Q_D^*) and secondarily on orbital dynamics. The classic distribution $\bar{n}(a) \propto a^{-q}$ with $q = 7/2$ (Dohnanyi 1969) assumes size-independent

impact strength and a steady-state, self-similar solution, i.e. extending to arbitrarily large and small sizes. However, Q_D^* , the energy per mass required to catastrophically disrupt a target (unbind half the mass), decreases with increasing size for small bodies in the strength-dominated regime. Above ~ 0.1 km, disruption is gravity-dominated, and Q_D^* increases with size.

A size-dependent Q_D^* affects the predicted q (O’Brien & Greenberg 2003). In the strength regime, large bodies are weaker and preferentially destroyed, steepening $\bar{n}(a)$ to larger q (and vice-versa in the gravity-dominated regime). The steady-state approximation is also inexact due to the gradual erosion of the source population. Combining these effects, Gáspár et al. (2012) calculate $q = 3.65$ in the strength-dominated regime, consistent with observed spectral energy distributions.

A break in the powerlaw q introduces non-self-similar effects, namely waves in the size distribution (Campo Bagatin et al. 1994; Thébault & Augereau 2007). For example when small grains are removed, an excess of slightly larger grains develops due to reduced collisional erosion. However this excess in turn produces a deficit of yet larger bodies. The wave pattern of alternating excesses and deficits eventually washes out with increasing size, due to the broad range of bullet-to-target mass ratios that can produce debris.

Most collisional size distributions fall between $3 < q < 4$ so that larger bodies incorporate most of the total mass while smaller bodies dominate the surface area. Small μm -size grains primarily emit infrared radiation and also scatter starlight. Millimeter-wave facilities (like ALMA) are sensitive to larger ($> 100\mu\text{m}$) grains. The different grain sizes in the collisional cascade also experience varying non-gravitational forces.

4.3. Non-gravitational forces on small particles

The large grains observed at mm and sub-mm wavelengths reside in orbits near the parent bodies that supply the collisional cascade. Smaller grains are more mobile, due to stronger non-gravitational forces, including radiation pressure, Poynting-Robertson drag, stellar wind drag, and Lorentz forces (Burns et al. 1979; Gustafson 1994).

Gravity and radiation pressure forces on dust grains are both inverse square laws, making their dimensionless ratio,

$$\beta = \left| \frac{F_r}{F_g} \right| = \frac{3L_* Q_{\text{PR}}}{16\pi GM_* c p a}, \quad (4)$$

useful, with Q_{PR} the scattering coefficient, G the gravitational constant, L_* the stellar luminosity, M_* its mass, and ρ the density of the grain. Radiation pressure reduces the effective gravitational force by a factor $1 - \beta$, and grains with $\beta \geq 1$ experience a repulsive radial force.

Expulsion occurs when the grain’s orbital speed exceeds the modified escape velocity from the system:

$$v_{\text{orb}} > v_{\text{esc}} = \sqrt{\frac{2GM_*}{R}(1 - \beta)}, \quad (5)$$

with R the orbital radius. Thus grains with $\beta \geq 0.5$ will pass very quickly out of the system on hyperbolic orbits, assuming grains are released at the the local circular Keplerian velocity (LCKV). Grains (starting at the LCKV) with $\beta < 0.5$ find themselves on eccentric orbits with periastrons at their release point. An initial kick that gives a deviation from the LCKV will give a different v_{orb} and critical β .

From the perspective of an orbiting grain, stellar radiation arrives from a slightly forward-shifted direction due to the aberration of light. Absorbed radiation imparts momentum that opposes the orbital motion, producing Poynting-Robertson drag (PRD). PRD causes inspiral of the grain towards the star and also damps the orbital eccentricity. Since the speed of light greatly exceeds orbital velocities, the aberration angle is small and the force weak:

$$F_{\text{PR}} = \frac{v}{c^2}W = \frac{a^2L_*}{4c^2} \sqrt{\frac{GM_*}{R^5}} \quad (6)$$

where v is the velocity of the grain, c the speed of light, and W the power of the incoming radiation.

PRD is more pronounced for smaller grains closer to their stars. The PRD force weakens with distance as $1/R^{2.5}$ vs. $1/R^2$ for gravity. The gravitational force varies with mass, $\propto a^3$, while $F_{\text{PR}} \propto a^2$. PRD is thus most significant just above the blow-out size ($\beta \lesssim 0.5$) and is already weak for millimeter-size grains. The inflow of dust from PRD is insufficient to sustain most observably bright inner disks (Wyatt 2008). Instead, this dust must be generated *in situ* (e.g., asteroid collisions) or be brought in by comets that disintegrate and deposit the dust.

Stellar wind drag is analogous to PRD, except it is caused by the impact of particles in the stellar wind onto the grain, with an analogous asymmetry in forces in the grain frame of

reference. Although usually similar to or weaker than PRD, this force can be dominant over PRD for very small grains close to a star (Minato et al. 2006) or around young and active late-type stars (Plavchan et al. 2005).

Lorentz forces, F_{Lor} , are generally negligible. However, near hot stars nanograins can acquire substantial electrical charges and can be retained close to the star to create small near-infrared excesses from hot (~ 1500 K) dust (Rieke et al. 2015).

5. Planetesimals and debris: common patterns

We might expect *planetesimal* systems to reflect the striking diversity of known *exoplanetary* systems. However, the hundreds of observed debris systems reveal striking similarities. Figure 4 illustrates the prevalent debris disk zones and Figure 5 shows an example.

5.1. *Very hot dust*

Within a few tenths of an AU of the Sun, only the most refractory grains can survive at temperatures ~ 1500 K. Moreover, grains in the $0.1 - 1\mu\text{m}$ size range are ejected by radiation pressure (Gustafson 1994). Nonetheless, a population of \sim nanometer-size grains exists, produced by grain-grain collisions and the sublimation of larger grains. These nanograins acquire electrical charge by electron impact and the photoelectric effect and are trapped in the Solar magnetic field by Lorentz forces (Mann et al. 2007). Some stars (mostly A-type) have much larger amounts of very hot dust lying within ~ 0.2 AU (e.g., Absil et al. 2013). The spectral energy distribution of this component falls steeply toward longer wavelengths, indicating a lack of grains larger than 200 nm in radius. Again, these grains are probably retained by Lorentz force (Rieke et al. 2015).

5.2. *Hot dust in the terrestrial planet zone*

Near the Earth, a very dilute population of dust scatters sunlight to yield the zodiacal light and emits primarily in the $10 - 20\mu\text{m}$ region. The $10\mu\text{m}$ silicate emission feature reveals that some of these hot (~ 300 K) grains are \sim micron-sized² (Ootsubo et al. 2009, see Figure

²As the size increases above a few microns, the silicate feature is rapidly reduced because the grain becomes optically thick (e.g., Papoular 1983).

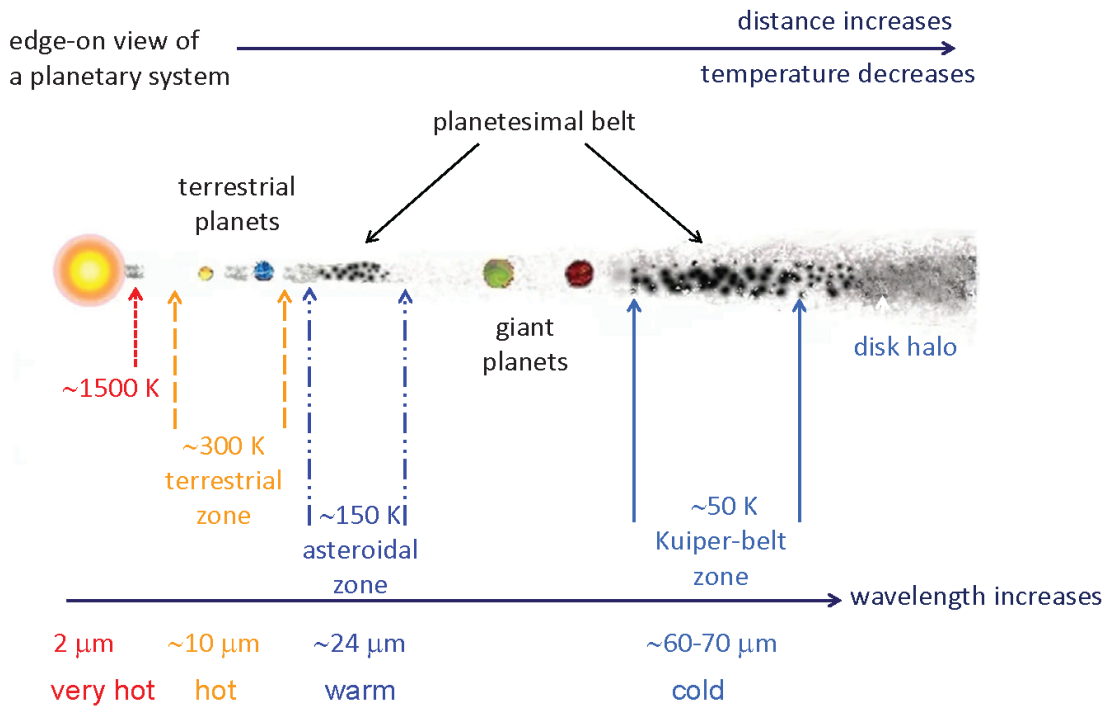


Fig. 4.— The five characteristic zones of debris disks; all zones are not detected in every disk (Su & Rieke 2014). The zones are products of temperature, not physical distance from the star, so higher luminosity (L_{star}) stars result in scaled-up dimensions, nominally in proportion to $\sqrt{L_{star}}$. For a given L_{star} , the nominal dust temperature decreases with distance, r_d , as $1/\sqrt{r_d}$.

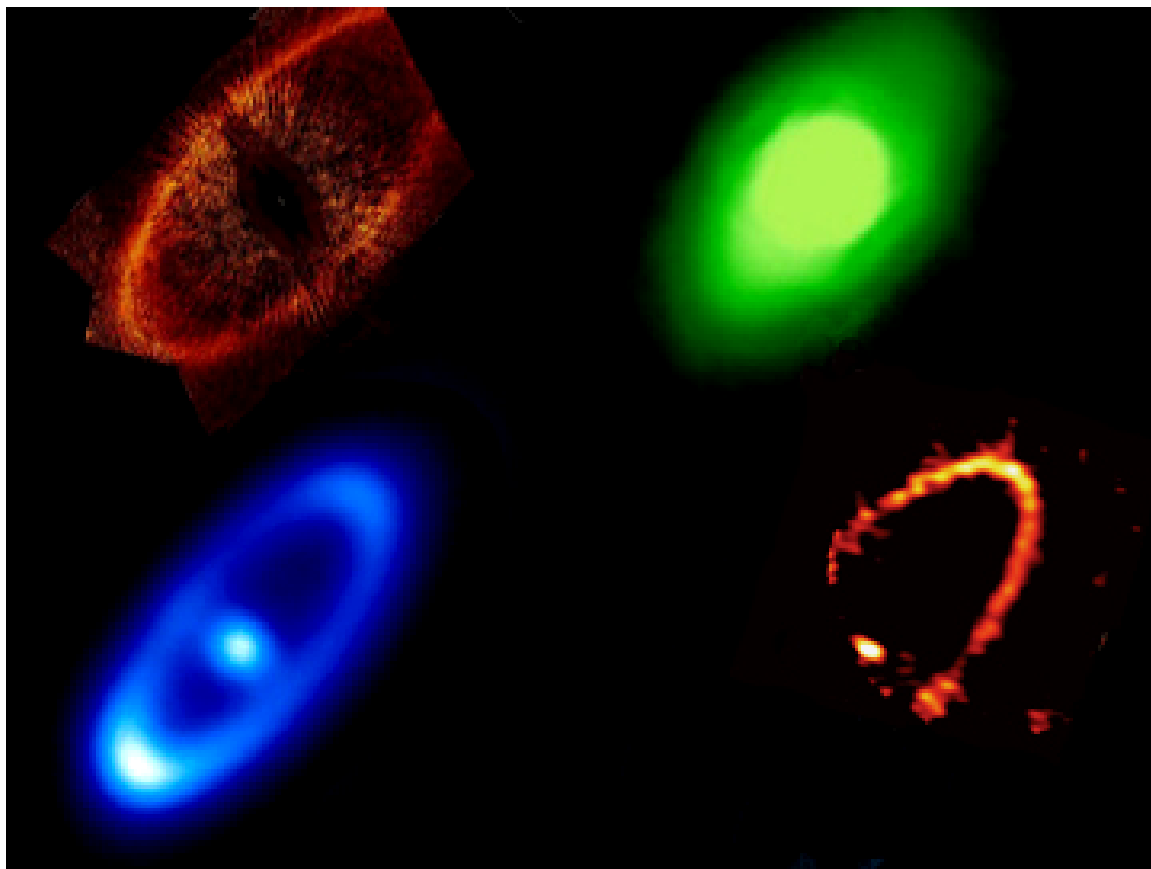


Fig. 5.— The archetypal debris disk around Fomalhaut. To the lower right, the ALMA image ($870\mu\text{m}$) shows the parent body ring (Boley et al. 2012). At $70\mu\text{m}$ (lower left, Herschel; Acke et al. 2012) the parent body ring is again prominent, with the star bright at the center (although the stellar signal is enhanced by a dust component); detailed analysis reveals a halo of β meteroids and escaping grains. At $24\mu\text{m}$ (upper right, Spitzer; Stapelfeldt et al. 2004), the resolution is only slightly poorer than at $70\mu\text{m}$, so structural differences are meaningful. The central peak of the debris system is about 20% of the total unresolved flux; the remaining 80% in this image is due to the star. The HST image (upper left; Kalas et al. 2013) is dominated by small grains efficient at scattering. They line the parent body belt inner edge and extend beyond out into the halo. [Credit: HST: NASA, ESA, P. Kalas, J. Graham, E. Chiang, E. Kite (University of California, Berkeley), M. Clampin (NASA GSFC), M. Fitzgerald (LLNL), and K. Stapelfeldt and J. Krist (NASA JPL); Spitzer: NASA, JPL-Caltech, K. Stapelfeldt (JPL); Herschel: ESA/Herschel/PACS/Bram Acke, KU Leuven, Belgium; ALMA: A.C. Boley (University of Florida, Sagan Fellow), M.J. Payne, E.B. Ford, M. Shabran (University of Florida), S. Corder (North American ALMA Science Center, National Radio Astronomy Observatory), and W. Dent (ALMA, Chile), NRAO/AUI/NSF]

6). However, the silicate feature is subtle; most of the dust is 10 - 40 μ m in size. The grain population is maintained by the disintegration of Jupiter Family Comets and the breakup of asteroids, with the inflow resulting mostly from PRD (Nesvorný et al. 2010). Hot dust is observed in many debris disks as subtle silicate emission features (Ballering et al. 2014; Mittal et al. 2015). In some cases, the hot dust component has been resolved (e.g., Mennesson et al. 2014); in the best-studied examples, the dust is relatively close to the star, inside the zone thermally equivalent to the orbit of the Earth (Stock et al. 2010; Defrère et al. 2015).

5.3. *Warm* (asteroidal) and *cold* (Kuiper Belt-like) dust

Going outward from the Sun, the first significant planetesimal/debris disk system is the asteroid belt, with dust produced primarily by the disintegration of Jupiter Family Comets (Nesvorný et al. 2010), but with a significant contribution from asteroid collisions. Indeed, dust bands in the zodiacal light trace the production of collisional asteroid families over the past ~ 10 Myr (Grogan et al. 2001; Nesvorný et al. 2003). The inflection in the asteroid size distribution near 25 km radius indicates that larger bodies are indestructible, while smaller ones participate in the collisional cascade (e.g., O’Brien & Sykes 2011). Still, the low volume density of asteroids gives a low fractional luminosity of dust emission, $L_{dust}/L_{star} \sim 10^{-7}$ (Nesvorný et al. 2010), nearly two orders of magnitude below detection limits around other stars (Roberge et al. 2012).

Continuing outward, there is a gap and then the Kuiper Belt debris disk, with a sharp inner edge shepherded by Neptune (Liou & Zook 1999) and resonant structures at larger radii (e.g., Adams et al. 2014). *In situ* dust sampling by the Student Dust Counter on the New Horizons mission (Szalay et al. 2015) confirms that the Kuiper Belt, despite the lower planetesimal surface density and faster orbits, is a venue for collisional-cascade-based dust production. The far-infrared emission from Kuiper Belt dust is estimated to be only about 1% of the Solar photospheric output at these wavelengths, below current detection limits around other stars (Vitense et al. 2012).

Like the Solar System, debris disks with warm components overwhelmingly come as two-temperature systems (Kennedy & Wyatt 2014): a far-infrared component with cold temperatures, 50–100K and a warm, 150–200 K, component (e.g., Ballering et al. 2013; Chen et al. 2014). Large planets could naturally clear the region between the dust belts (e.g., Su et al. 2013). The warm components fade in ~ 300 Myr (Gáspár et al. 2013); the majority of debris disks are detected only as a cold excess. Bright far infrared excesses, in comparison, persist for about 3.5 GYr and are seen roughly independently of stellar type at the 20% level around stars of late F through early K (Sierchio et al. 2014). These outer

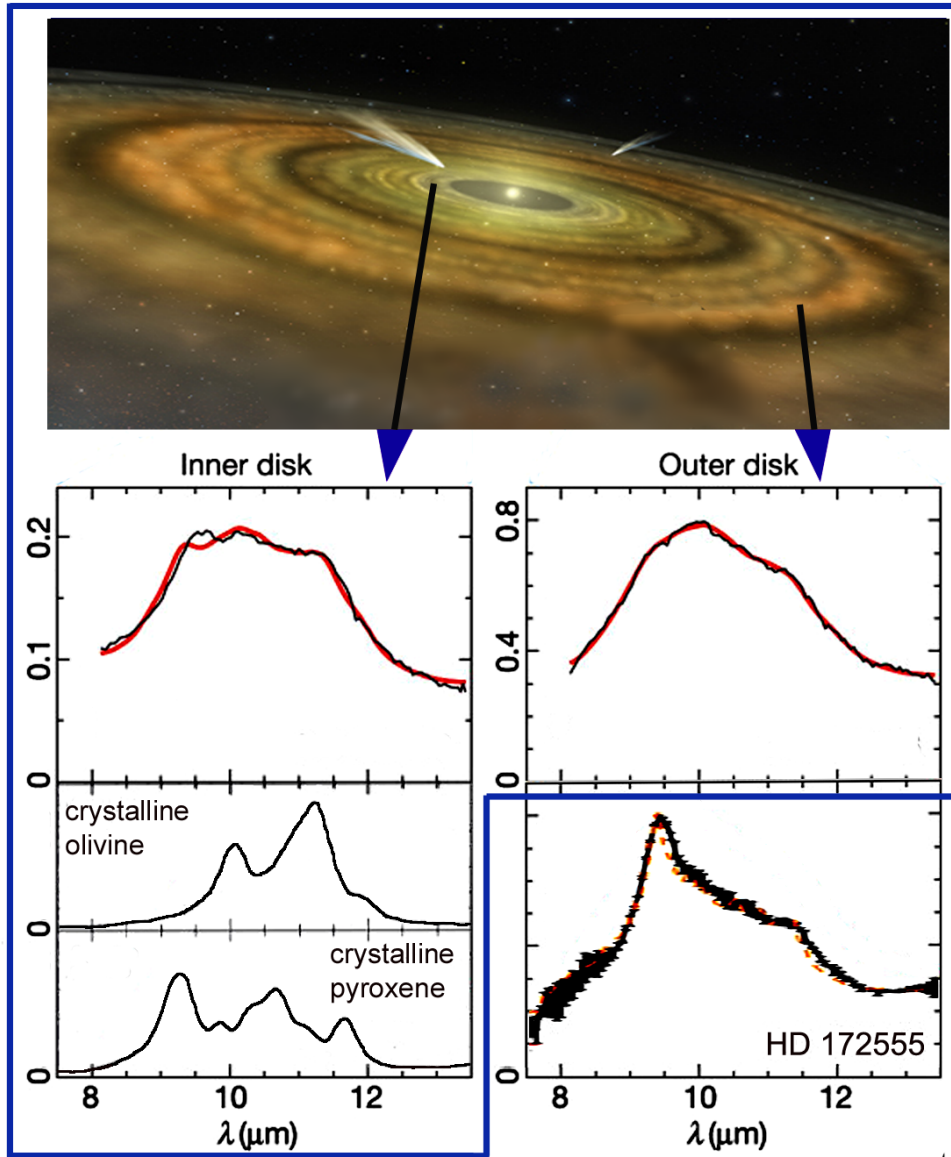


Fig. 6.— Silicate emission varies with the location in, and evolutionary state of, debris disks. The top image schematically represents a young debris disk. The hot inner disk of HD 163296 (middle left; spectrum in black, model in red) shows silicate emission. The model contains olivine and pyroxene silicates in crystalline form, as expected for high temperatures (lower left); however, grain growth washes out some spectral features. The outer disk has a smooth $10\mu\text{m}$ peak (middle right), well fit by unprocessed amorphous silicates. [Credit: NASA/FUSE/Lynette Cook, van Boekel et al. (2004)]. HD 172555 (lower right) shows a sharp $9\mu\text{m}$ feature, characteristic of silica grains recently condensed from vapor (Johnson et al. 2012).

belts are also accessible to scattered-light imaging, from which we have obtained the highest resolution images of the small dust distributions (e.g., Schneider et al. 2014; Soummer et al. 2014).

The similar locations of the Kuiper Belt and outer debris disks suggests that massive planets also reside in debris systems. The situation for the asteroid belt is more complex. It overlaps with plausible locations for the snow line in the Sun’s protoplanetary disk (Kennedy & Kenyon 2008). Pressure enhancements at the snow line can provide a favorable site for planetesimal formation, see §2. But why would such planetesimals fail to assemble into more massive planets, given that the primordial asteroid belt was two to three orders of magnitude more massive than today (Morbidelli et al. 2015a)? Somehow, an early-formed Jupiter limited planetesimal growth and/or ejected most asteroids. In the Grand Tack scenario, Jupiter may even have migrated inwards through the belt to the location of Mars and then back out (Walsh et al. 2011), strongly affecting the structure of the belt. It is thought that the asteroid belt then reformed from bodies inside and outside of its current location (Walsh et al. 2012). Alternatively, warm debris might indicate the disintegration of huge comet populations, analogous to Jupiter Family Comets.

5.4. Dust halos

Outside the Kuiper Belt there must be a dilute halo of small grains whose motions are strongly affected by radiation pressure - both β meteoroids on highly elliptical marginally bound orbits, and also particles escaping into interstellar space. Similar but far more dramatic halos are detected around a number of prominent debris disks such as β Pic (Augereau et al. 2001) and Fomalhaut (Figure 5), in scattered light as well as thermal emission.

6. Evolution of planetesimal systems

Many exoplanetary systems become virtually invisible after their natal protoplanetary disks dissipate, by about 10 Myr of age. The similarities in the Solar System and exoplanetary debris disks embolden us to use debris disks to reveal the development of the invisible exoplanetary systems themselves. Debris disks complement radial velocity and transit studies, which focus on the inner regions of mature planetary systems.

The *Kepler* mission revealed that planets within only 0.5 AU of G, K and especially M stars outnumber the stars themselves (Youdin 2011b; Mulders et al. 2015; Dressing & Charbonneau 2015). In contrast to this bounty, the mass in protoplanetary disks – inferred

from dust observations – is not overly generous (Williams & Cieza 2011). Significant early coagulation into larger grains avoids an outright conflict with the large incidence of planetary systems (Sheehan & Eisner 2014).

The most common planets appear to have masses between Earth and Neptune (e.g., Malhotra 2015), far below direct detection limits (i.e., imaging). Such unseen planets leave traces in debris disks; for example, within the Solar System, the inner edge of the Kuiper Belt is shepherded by Neptune (Liou & Zook 1999). Gaps between warm and cold debris belts can also be explained by intervening planets, allowing some understanding of their incidence.

Debris disks can also trace several phases in planetary system evolution, including: 1.) violent dynamical activity during terrestrial planet growth; 2.) gradual erosion of remnant belts of planetesimals; and 3.) late phase bursts of activity caused by orbital instabilities among planets, such as the Late Heavy Bombardment in the Solar System.

6.1. Formation of terrestrial planets

Terrestrial planets may begin their assembly during the protoplanetary disk phase, with the rapid accretion of pebbles and boulder-sized solids (e.g., Morbidelli et al. 2015b). Aerodynamic drift brings solids from the outer disk, while gas drag also enhances the capture probability of large pebbles (Ormel & Klahr 2010).

For traditional planetesimal-dominated accretion, however, the isolation mass plays a key role. It is reached when protoplanets have accreted most of the planetesimals in their feeding zones (Youdin & Kenyon 2012), marking the endpoint of the rapid phase of oligarchic planetesimal accretion (Kokubo & Ida 1998). Earth and Venus are much larger than the isolation mass; the merger of isolated oligarchs into such planets requires another 10-100 Myr of intermittent giant impacts (Chambers 2004; Kenyon & Bromley 2006; Kleine et al. 2009), like the Moon-forming impact when the Solar System was 30–100 Myr old (e.g., Jacobson et al. 2014). Debris disks can trace this process via the high rate of collisional grinding of planetesimals stirred by growing terrestrial protoplanets (Kenyon & Bromley 2004) and also by the large amounts of dust produced in individual violent collisions, some of it condensed directly from vaporized rock.

Violent impacts during this era are revealed by the $9\mu\text{m}$ silica emission feature, see Figure 6. Silica dust can condense directly from gas produced from silicate minerals in violent collisions (Johnson & Melosh 2012); gaseous silica was a major product of the collision that formed our Moon (Canup 2004). HD 172555, a member of the 20 Myr-old (Soderblom et al.

2014) β Pic moving group, is an outstanding example of a disk with a strong silica feature (Lisse et al. 2009). Johnson et al. (2012) conclude that the dust is produced at ~ 6 AU from the star; given the luminosity of HD 172555, this distance is thermally equivalent to about 2 AU in the Solar System, i.e., just outside the orbit equivalent to that of Mars.

Jackson & Wyatt (2012) concluded that the aftermath of the Moon-forming collision was a circumsolar ring of debris detectable (with current infrared astronomy technology from a nearby planetary system) for up to 25 Myr. Even greater variability has been seen in the most extreme debris systems (Melis et al. 2012; Meng et al. 2012, 2015). For example, the star ID8 in the 35 Myr old NGC 2547 cluster changes its output on monthly timescales (Meng et al. 2014). The debris orbits at ~ 0.33 AU from a star similar in luminosity to the sun, i.e., near the equivalent position of Mercury. Both HD 172555 and ID8 are estimated to have about 1×10^{19} kg of finely divided dust, indicating asteroids at least 200 km in diameter must have been destroyed around them. More evidence for violent events in the era of terrestrial planet formation comes from ALMA studies of β Pic in the $J = 3-2$ transition of ^{12}CO (Dent et al. 2014). The massive gas cloud on (only) one side of the disk could arise either from the outward migration of a planet that locally enhances planetesimal collisions, or from debris of a single recent planetesimal collision.

6.2. Long term dust production

After the mayhem of planet formation has passed, debris disks continue to produce lower levels of dust. As the population of destructible planetesimals is eroded, dust production from collisional cascades decays with time (e.g., Wyatt et al. 2007). Since collision rates are proportional to the instantaneous mass of the debris disk, this fading is nearly independent of the disk mass; more massive disks simply undergo a brief initial phase of rapid collisional destruction. The time evolution of debris disk emission is consistent with this premise (Gáspár et al. 2013), assuming a distribution of initial disk masses proportional to that of protoplanetary disks. This behavior provides a simple baseline against which to identify deviations.

6.3. Late stage dynamical shakeups

Anomalously large excesses likely reflect a dynamical shakeup of the planetary system and enhanced gravitational stirring of its planetesimals. There is a residual (a few %) of disks detected at $24\mu\text{m}$ well beyond the age of ~ 600 Myr when the baseline would predict no

more activity (Gáspár et al. 2013). Many of these systems show features in their mid-infrared spectra indicating very small dust grains with short lifetimes around their stars, indicating recent collisions producing enhanced levels of dust. Breaking up a Ceres-sized planetesimal should yield a detectable excess at $24\mu\text{m}$ for about 1 million years (Kral et al. 2015).

More extensive dynamical activity has more profound effects. Booth et al. (2009) simulated the effect of the Late Heavy Bombardment (in the context of the Nice model) on the history of the Solar System’s debris disk. The $24\mu\text{m}$ emission spikes by a factor of ~ 3 , but rapidly fades below detection limits in ~ 30 Myr. The $70\mu\text{m}$ emission does not spike but remains detectable much longer, >300 Myr.

7. Conclusion

Planetesimals are the building blocks of planet systems. We are developing an understanding of how they are formed and grow in their first 10 Myr, although substantial questions remain such as: 1.) how far past mm-sizes does collisional growth proceed (at different locations) during the lifetime of protoplanetary disks; and 2.) what combination of dynamical processes (e.g. streaming instabilities, pressure traps and gravitational instabilities) complete the growth of planetesimals if/when standard collisional growth stalls. Past this era, we can trace planetesimal evolution through debris disks, from which we have found:

- There is a remarkable similarity in the positions of the planetesimal belts in the Solar System and around other stars.
- This layout probably reflects the influence of unseen giant planets in the exoplanetary systems.
- Debris disks exhibit the processes in the building of terrestrial planets through a.) spectral features indicative of the generation of silica dust in violent collisions; and b.) variability in dust production reflecting ongoing planetesimal collisions.
- Although most debris disks fade away in accordance with theoretical expectations, a few percent are found around older stars and indicate late phases of dynamical activity in their planet systems.

REFERENCES

- Absil, O., Defrère, D., Coudeè du Foresto, V., Di Folco, E. et al. 2013. A near-infrared interferometric survey of debris-disc stars. III. First statistics based on 42 stars observed with CHARA/FLUOR. *A&A*, 555, 104.
- Acke, B., Min, M., Dominik, C. et al. 2012. Herschel images of Fomalhaut. An extrasolar Kuiper belt at the height of its dynamical activity. *A&A*, 540, 125.
- Adachi, I., Hayashi, C., & Nakazawa, K. 1976. The gas drag effect on the elliptical motion of a solid body in the primordial solar nebula. *Prog. Theor. Phys.*, 56, 1756.
- Adams, E. R., Gulbis, A. A. S., Elliot, J. L. et al. 2014. De-biased populations of Kuiper Belt Objects from the Deep Ecliptic Survey. *AJ*, 148, 55.
- ALMA Partnership, Brogan, C.L., Perez, L.M. et al. 2015. The 2014 ALMA long baseline campaign: first results from high angular resolution observations toward the HL Tau region. *ApJL*, 808, 3.
- Augereau, J. C., Nelson, R. P., Lagrange, A. M. et al. 2001. Dynamical modeling of large scale asymmetries in the beta Pictoris dust disk. *A&A*, 370, 447.
- Aumann, H. H., Beichman, C. A., Gillett, F. C. et al. 1984. Discovery of a shell around Alpha Lyrae, *ApJL*, 278, 23.
- Bai, X.-N. and Stone, J. M. 2010. The effect of the radial pressure gradient in protoplanetary disks on planetesimal formation. *ApJL*, 722, 220.
- Ballering, N. P., Rieke, G. H., Su, K. Y. L., & Montiel, E. 2013. A trend between cold debris disk temperature and stellar type: implications for the formation and evolution of wide-orbit planets. *ApJ*, 775, 55.
- Ballering, N. P., Rieke, G. H., & Gáspár, A. 2014. Probing the terrestrial regions of planetary systems: warm debris disks with emission features. *ApJ*, 793, 57.
- Beitz, E., Güttler, C., Blum, J., Meisner, T., Teiser, J., & Wurm, G. 2011. Low-velocity collisions of centimeter-sized dust aggregates. *ApJ*, 736, 34.
- Blum, J. and Wurm, G. 2008. The growth mechanisms of macroscopic bodies in protoplanetary disks. *ARA&A*, 46, 21.
- Boley, A. C., Payne, M. J., Corder, S. et al. 2012. Constraining the planetary system of Fomalhaut using high-resolution ALMA observations. *ApJL*, 750, 21.

- Booth, M., Wyatt, M. C., Morbidelli, A., Moro-Martín, A., & Levison, H. F. 2009. The history of the Solar system’s debris disc: observable properties of the Kuiper belt. *MNRAS*, 399, 385.
- Burns, J. A., Lamy, P. L., & Soter, S. 1979. Radiation forces on small particles in the solar system. *Icarus*, 40, 1.
- Campo Bagatin, A., Cellino, A., Davis, D. R., Farinella, P., & Paolicchi, P. 1994. Wavy size distributions for collisional systems with a small-size cutoff. *Planet. Space Sci.*, 42, 1079.
- Canup, R. M. 2004. Simulations of a late lunar-forming impact. *Icarus*, 168, 433
- Carrera, D., Johansen, A., & Davies, M. B. 2015. How to form planetesimals from mm-sized chondrules and chondrule aggregates. *A&A*, 579A, 43.
- Chambers, J. E. 2004. Planetary accretion in the inner Solar System. *Earth Plan. Sci. Let.*, 223, 241.
- Chen, C. H., Mittal, T., Kuchner, M. et al. 2014. The Spitzer Infrared Spectrograph Debris Disk Catalog. I. Continuum analysis of unresolved targets. *ApJS*, 211, 25.
- Chiang, E. & Youdin, A. N. 2010. Forming planetesimals in Solar and extrasolar nebulae. *Annual Review of Earth and Planetary Sciences*, 38, 93.
- Cuzzi, J. N., Hogan, R. C., & Shariff, K. 2008. Toward planetesimals: dense chondrule clumps in the protoplanetary nebula. *ApJ*, 687, 1432.
- Defrère, D., Hinz, P. M., Skemer, A. J. et al. 2015. First-light LBT nulling interferometric observations: warm exozodiacal dust resolved within a few AU of η Crv. *ApJ*, 799, 42.
- Dent, W. R. F., Wyatt, M. C., Roberge, A. et al. 2014. Molecular gas clumps from the destruction of icy bodies in the β Pictoris debris disk. *Science*, 343, 1490.
- Dohnanyi, J. S. 1969. Collisional model of asteroids and their debris. *J. Geophys. Res.*, 74, 2531.
- Drażkowska, J., Windmark, F., & Dullemond, C. P. 2014. Modeling dust growth in protoplanetary disks: The breakthrough case. *A&A*, 567, A38.
- Dressing, C. D., & Charbonneau, D. 2015. The occurrence of potentially habitable planets orbiting M Dwarfs estimated from the full Kepler dataset and an empirical measurement of the detection sensitivity. *ApJ*, 807, 45.

- Gáspár, A., Psaltis, D., Rieke, G. H., & Özel, F. 2012. Modeling collisional cascades in debris disks: steep dust-size distributions. *ApJ*, 754, 74.
- Gáspár, A., Rieke, G. H., & Balog, Z. 2013. The collisional evolution of debris disks. *ApJ*, 768, 25.
- Gladman, B., Kavelaars, J. J., Petit, J.-M. et al. 2001. The structure of the Kuiper Belt: size distribution and radial extent. *AJ*, 122, 1051.
- Goldreich, P. & Ward, W. R. 1973. The formation of planetesimals. *ApJ*, 183, 1051.
- Goodman, J. and Pindor, B. 2000. Secular instability and planetesimal formation in the dust layer. *Icarus*, 148, 537.
- Grogan, K., Dermott, S. F., & Durda, D. D. 2001. The size-frequency distribution of the Zodiacal Cloud: evidence from the Solar System dust bands. *Icarus*, 152, 251.
- Gustafson, B.Å.S. 1994. Physics of Zodiacal dust. *AREPS*, 22, 553.
- Jackson, A. P. & Wyatt, M. C. 2012. Debris from terrestrial planet formation: the Moon-forming collision. *MNRAS*, 425, 657.
- Jacobson, S. A., Morbidelli, A., Raymond, S. N., O’Brien, D. P., Walsh, K. J., & Rubie, D. C. 2014. Highly siderophile elements in Earth’s mantle as a clock for the Moon-forming impact. *Nature*, 508, 84.
- Jacquet, E., Balbus, S., & Latter, H. 2011. On linear dust-gas streaming instabilities in protoplanetary discs. *MNRAS*, 415, 3591
- Jewitt, D., & Luu, J. 1993. Discovery of the candidate Kuiper Belt object 1992 QB1. *Nature*, 362, 730.
- Johansen, A. and Youdin, A. N. 2007. Protoplanetary disk turbulence driven by the streaming instability: nonlinear saturation and particle concentration. *ApJ*, 662, 627
- Johansen, A., Youdin, A. N., & Lithwick, Y. 2012. Adding particle collisions to the formation of asteroids and Kuiper belt objects via streaming instabilities. *A&A*, 537, A125.
- Johansen, A., MacLow, M.-M., Lacerda, P., & Bizzarro, M. 2015b. Growth of asteroids, planetary embryos, and Kuiper belt objects by chondrule accretion. *Sci. Adv.*, 115109.
- Johansen, A., Jacquet, E., Cuzzi, J. N., Morbidelli, A., & Gounelle, M. 2015a. New paradigms For asteroid formation. arXiv:1505.02941.

- Johnson, B. C., & Melosh, H. J. 2012. Formation of spherules in impact produced vapor plumes. *Icarus*, 217, 416.
- Johnson, B. C., Lisse, C. M., Chen, C. H. et al. 2012. A self-consistent model of the circumstellar debris created by a giant hypervelocity impact in the HD 172555 system. *ApJ*, 761, 45.
- Kalas, P., Graham, J. R., Fitzgerald, M. P., & Clampin, M. 2013. STIS coronagraphic imaging of Fomalhaut: main belt structure and the orbit of Fomalhaut b. *ApJ*, 775, 56.
- Kennedy, G. M., & Kenyon, S. J. 2008. Planet formation around stars of various masses: The snow line and the frequency of giant planets. *ApJ*, 673, 502.
- Kennedy, G. M., & Wyatt, M. C. 2014. Do two-temperature debris discs have multiple belts?. *MNRAS*, 444, 3164.
- Kenyon, S. J. & Bromley, B. C. 2004. Detecting the dusty debris of terrestrial planet formation. *ApJL*, 602, 133.
- Kenyon, S. J. & Bromley, B. C. 2006. Prospects for detection of catastrophic collisions in debris disks. *AJ*, 131, 1837.
- Kenyon, S. J. & Bromley, B. C. 2012. Coagulation calculations of icy planet formation at 15-150 AU: a correlation between the maximum radius and the slope of the size distribution for trans-Neptunian objects. *AJ*, 143, 63.
- Kleine, T., Touboul, M., Bourdon, B., et al. 2009. Hf-W chronology of the accretion and early evolution of asteroids and terrestrial planets. *Geochim. Cosmochim. Acta*, 73, 5150.
- Kokubo, E. & Ida, S. 1998. Oligarchic growth of protoplanets. *Icarus*, 131, 171.
- Kral, Q., Thébault, P., Augereau, J.-C., Boccaletti, A., & Charnoz, S. 2015. Oligarchic growth of protoplanets. *A&A*, 573, 39.
- Kretke, K. A. & Lin, D. N. C. 2007. Grain retention and formation of planetesimals near the snow line in MRI-driven turbulent protoplanetary disks. *ApJL*, 664, 55.
- Liou, J.-C., & Zook, H. A. 1999. Signatures of the giant planets imprinted on the Edgeworth-Kuiper Belt dust disk. *AJ*, 118, 580.

- Lisse, C. M., Chen, C. H., Wyatt, M. C. et al. 2009. Abundant circumstellar silica dust and SiO gas created by a giant hypervelocity collision in the 12 Myr HD172555 system. *ApJ*, 701, 2019.
- Lyra, W. & Lin, M.-K. 2013. Steady state dust distributions in disk vortices: observational predictions and applications to transitional disks. *ApJ*, 775, 17.
- Malhotra, R. 2015. The mass distribution function of planets. *ApJ*, 808, 71.
- Mann, I., Murad, E., & Czechowski, A. 2007. Nanoparticles in the inner Solar System. *Plan. Spc. Sci*, 55, 1000.
- Melis, C., Zuckerman, B., Rhee, J. H. et al. 2012. Rapid disappearance of a warm, dusty circumstellar disk. *Nature*, 487, 74.
- Meng, H. Y. A., Rieke, G. H., Su, K. Y. L. et al. 2012. Variability of the infrared excess of extreme debris disks. *ApJL*, 751, 17.
- Meng, H. Y. A., Su, K. Y. L., Rieke, G. H. 2014. Large impacts around a solar-analog star in the era of terrestrial planet formation. *Science*, 345, 1032.
- Meng, H. Y. A., Su, K. Y. L., Rieke, G. H. et al. 2015. Planetary collisions outside the Solar System: time domain characterization of extreme debris disks. *ApJ*, 805, 77.
- Mennesson, B., Millan-Gabet, R., Serabyn, E. et al. 2014. Constraining the exozodiacal luminosity function of main-sequence stars: complete results from the Keck Nuller mid-infrared surveys. *ApJ*, 797, 119.
- Minato, T., Köhler, M., Kimura, H., Mann, I., & Yamamoto, T. 2006. Momentum transfer to fluffy dust aggregates from stellar winds. *A&A*, 452, 701.
- Mittal, T., Chen, C. H., Jang-Condell, H. et al. 2015. The Spitzer Infrared Spectrograph Debris Disk Catalog. II. silicate feature analysis of unresolved targets. *ApJ*, 798, 87.
- Morbidelli, A., Walsh, K. J., O’Brien, D. P., Minton, D. A., & Bottke, W.F. 2015a. The dynamical evolution of the asteroid belt. arXiv:1501.06204.
- Morbidelli, A., Lambrechts, M., Jacobson, S., & Bitsch, B. 2015b. The great dichotomy of the Solar System: Small terrestrial embryos and massive giant planet cores. *Icarus*, 258, 418.
- Mulders, G. D., Pascucci, I., & Apai, D. 2015. An Increase in the Mass of Planetary Systems around Lower-mass Stars. *ApJ*, 814, 130

- Nesvorný, D., Bottke, W. F., Levison, H. F., & Dones, L. 2003. Recent origin of the Solar System dust bands. *ApJ*, 591, 486.
- Nesvorný, D., Jenniskens, P., Levison, H. A., Bottke, W. F., Vokrouhlický, D., & Gounelle, M. 2010. Cometary origin of the zodiacal cloud and carbonaceous micrometeorites. implications for hot debris disks. *ApJ*, 713, 816.
- O’Brien, D. P., & Greenberg, R. 2003. Steady-state size distributions for collisional populations: analytical solution with size-dependent strength. *Icarus*, 164, 334.
- O’Brien, D. P., & Sykes, M. V. 2011. The origin and evolution of the asteroid belt implications for Vesta and Ceres. *Spc. Sci. Rev.*, 163, 11.
- Ootsubo, T., Ueno, M., Ishiguro, M. et al. 2009. Mid-Infrared spectrum of the zodiacal light observed with AKARI/IRC. *ASP Conf. Ser.*, 418, 395.
- Ormel, C.W. and Klahr, H.H. 2010, The effect of gas drag on the growth of protoplanets., *A&A*, 520A, 43.
- Pan, L., Padoan, P., Scalo, J., Kritsuk, A. G., & Norman, M. L. 2011. Turbulent clustering of protoplanetary dust and planetesimal formation. *ApJ*, 740, 6.
- Papoular, R., & Pégourié, B. 1983. The IR silicate features as a measure of grain size in circumstellar dust. *A&A*, 128, 335.
- Plavchan, P., Jura, M., & Lipsky, S. J. 2005. Where are the M dwarf disks older than 10 million years?. *ApJ*, 631, 1161.
- Rieke, G. H., Gáspár, A., & Ballering, N. P. 2015. Magnetic grain trapping and the hot excesses around early-type stars. arXiv:1511.04998, *ApJ*, *accepted*.
- Roberge, Aki, Chen, C. H., Millan-Gabet, R. et al. 2012. The exozodiacal dust problem for direct observations of exo-earths. *PASP*, 124, 799.
- Schneider, G., Grady, C. A., Hines, D. C., et al. 2014. Probing for exoplanets hiding in dusty debris disks: disk imaging, characterization, and exploration with HST/STIS multi-roll coronagraphy. *AJ*, 148, 59
- Shariff, K. and Cuzzi, J. N. 2011. Gravitational instability of solids assisted by gas drag: slowing by turbulent mass diffusivity. *ApJ*, 738, 73.
- Sheehan, P. D., & Eisner, J. A. 2014. Constraining the disk masses of the class I binary protostar GV Tau. *ApJ*, 791, 19.

- Sierchio, J. M., Rieke, G. H., Su, K. Y. L., & Gáspár, A. 2014. The decay of debris disks around Solar-type stars. *ApJ*, 785, 33.
- Simon, J. B., Armitage, P. J., Li, R., & Youdin, A. N. The initial mass and size distribution of planetesimals. I. the effect of resolution, gravity, and initial conditions in streaming instability calculations. 2015, arXiv:1512.00009.
- Smith, B. A., & Terrile, R. J. 1984. A circumstellar disk around Beta Pictoris. *Science*, 226, 1421.
- Soderblom, D. R., Hillenbrand, L. A., Jeffries, R. D., Mamajek, E. E., & Naylor, T. 2014. Ages of young stars. in *Protostars & Planets VI*, ed. H. Beuther, R.S. Klessen, C.P. Dullemond, & T. Henning, UA Press: Tucson, pp 219-241.
- Soummer, R., Perrin, M. D., Pueyo, L. et al. 2014. Five debris disks newly revealed in scattered light from the Hubble Space Telescope NICMOS archive. *ApJL*, 786, 23.
- Stapelfeldt, K. R., Holmes, E. K., Chen, C. H. et al. 2004. First Look at the Fomalhaut debris disk with the Spitzer Space Telescope. *ApJS*, 154, 458.
- Stock, N. D., Su, K. Y.L., Liu, W. et al. 2010. The structure of the β Leonis debris disk. *ApJ*, 724, 1238.
- Su, K. Y. L., Rieke, G. H., Malhotra, R., et al. 2013. Asteroid belts in debris disk twins: Vega and Fomalhaut. *ApJ*, 763, 118.
- Su, K. Y. L., & Rieke, G. H. 2014. Signposts of multiple planets in debris disks. *IAU Symp.*, 299, 318.
- Szalay, J., Piquette, M., & Horanyi, M. 2015. Dust measurements by the Student Dust Counter onboard the New Horizons Mission to Pluto. *Lun. Plan. Inst.*, 1832, 1701.
- Takahashi, S. Z. and Inutsuka, S.-I. 2014. Two-component secular gravitational instability in a protoplanetary disk: a possible mechanism for creating ring-like structures. *ApJ*, 794, 55.
- Thébaud, P. & Augereau, J.-C. 2007. Collisional processes and size distribution in spatially extended debris discs. *A&A*, 472, 169.
- van Boekel, R., Min, M., Leinert, Ch, et al. 2004. The building blocks of planets within the ‘terrestrial’ region of protoplanetary disks. *Nature*, 432, 479.

- Vitense, Ch, Krivov, A. V., Kobayashi, H., & Löhne, T. 2012. An improved model of the Edgeworth-Kuiper debris disk. *A&A*, 540, 30.
- Walsh, K. J., Morbidelli, A., Raymond, S. N., O’Brien, D. P., & Mandell, A. M. 2011. A low mass for Mars from Jupiter’s early gas-driven migration. *Nature*, 475, 206.
- Walsh, K. J., Morbidelli, A., Raymond, S. N., O’Brien, D. P., & Mandell, A. M. 2012. Populating the asteroid belt from two parent source regions due to the migration of giant planets “The Grand Tack”. *Meteor. & Plan. Sci.*, 47, 1941.
- Weidenschilling, S.J. 1980, Dust to planetesimals - Settling and coagulation in the solar nebula. *Icarus*, 44, 172
- Weissman, P. R. 1984. The VEGA particulate shell - comets or asteroids? *Science*, 224, 987.
- Whipple, F. L. 1972. On certain aerodynamic processes for asteroids and comets. in *From Plasma to Planet*, Ed. Elvius, A., Wiley: New York, p 211.
- Williams, J. P. and Cieza, L. A. 2011. Protoplanetary disks and their evolution. *ARA&A*, 49, 67.
- Wyatt, M. C., Smith, R., Su, K. Y. L. et al. 2007. Steady State evolution of debris disks around A stars. *ApJ*, 663, 365.
- Wyatt, M. C. 2008. Evolution of debris disks. *ARA&A*, 46, 339.
- Youdin, A. N. 2010. From grains to planetesimals, ESA, Ed. T. Montmerle, D. Ehrenreich, & A.-M. Lagrange, 41, 187.
- . 2011. On the formation of planetesimals via secular gravitational instabilities with turbulent stirring, *ApJ*, 731, 99.
- . 2011b, The Exoplanet Census: A General Method Applied to Kepler, *ApJ*, 742, 38
- Youdin, A. N., & Chiang, E. I. 2004. Particle pileups and planetesimal formation. *ApJ*, 601, 1109.
- Youdin, A. N. and Goodman, J. 2005. Streaming instabilities in protoplanetary disks. *ApJ*, 620, 459.
- Youdin, A. N. & Johansen, A. 2007. Protoplanetary disk turbulence driven by the streaming instability: linear evolution and numerical methods. *ApJ*, 662.

- Youdin, A. N., & Kenyon, S. J. 2012. From disks to planets. in *Planets, Stars and Stellar Systems* ed. T. D. Oswalt, L. M. French, P. Kalas, Springer: Dordrecht, pp 1-62.
- Youdin, A. N., & Lithwick, Y. 2007. Particle stirring in turbulent gas disks: Including orbital oscillations. *Icarus*, 192, 588.
- Youdin, A. N. & Shu, F. H. 2002. Planetesimal formation by gravitational instability. *ApJ*, 580, 494.
- Zsom, A., Ormel, C. W., Güttler, C., Blum, J. & Dullemond, C. P. 2010. The outcome of protoplanetary dust growth: pebbles, boulders, or planetesimals? II. Introducing the bouncing barrier. *A&A*, 513A, 57.